

SUPPLEMENTARY INFORMATION

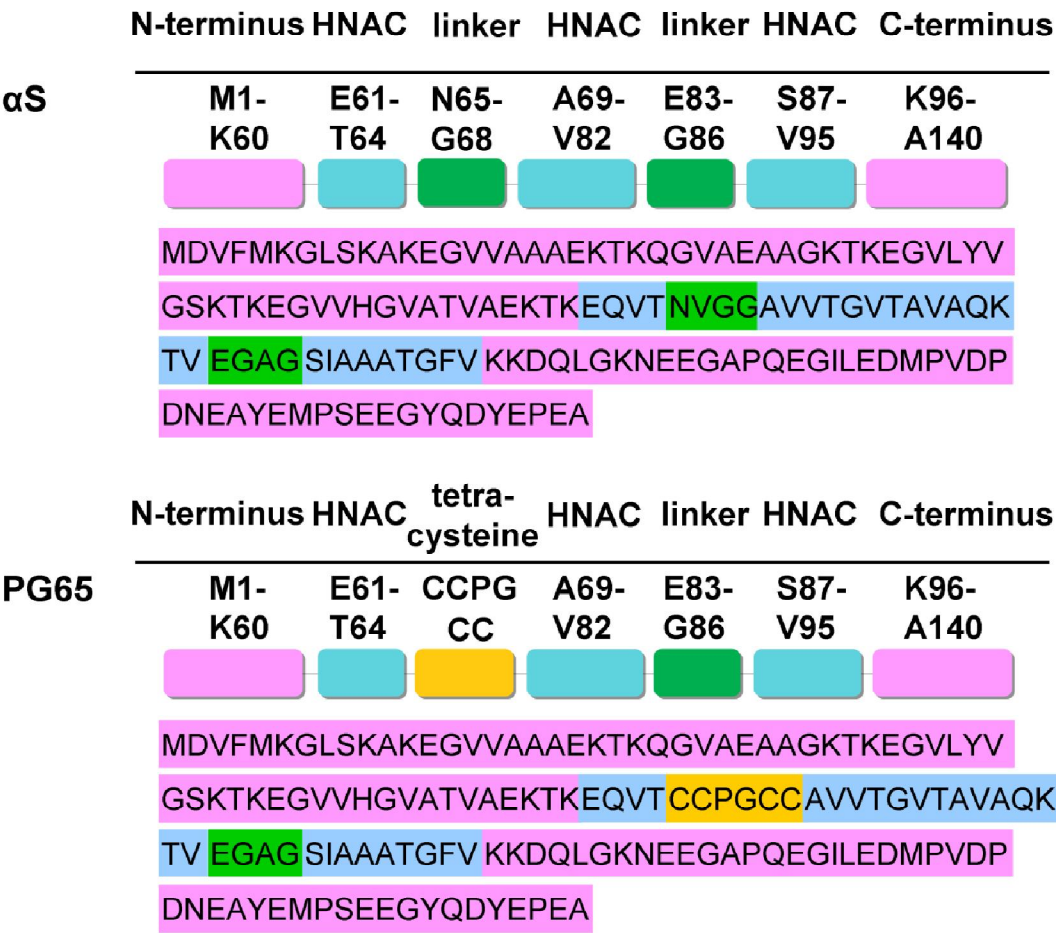


Fig. S1. The amino acid sequences of αS and PG65 along with their respective sequence schematics. Amino acids sequences were colored according to sequence schematics. Note that αS does not contain any cysteine residues.

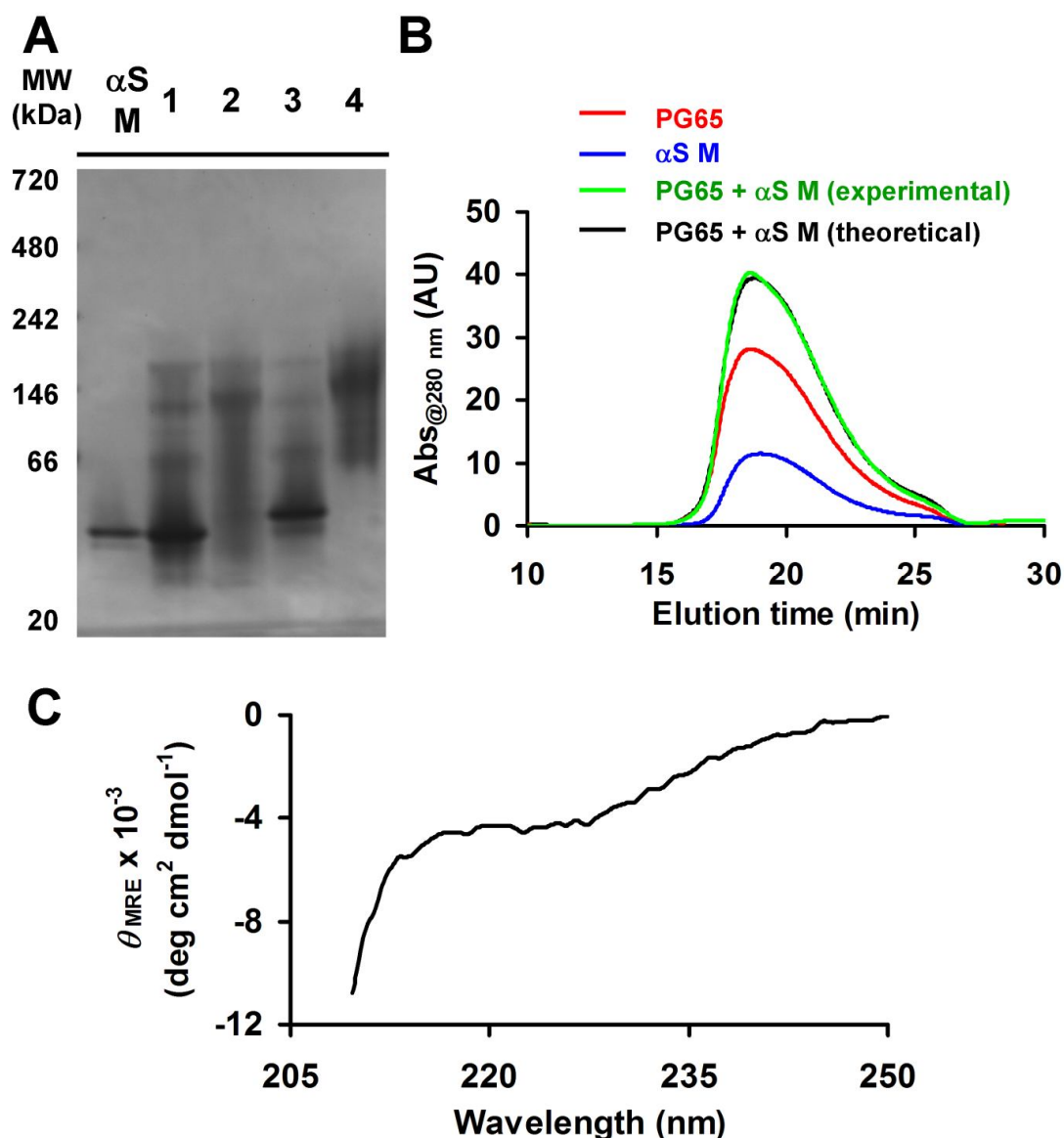


Fig. S2 (A) Native-PAGE of PG65 (lane 1), PG65F (lane 2), PG83 (lane 3) and PG83F (lane 4) at 35  $\mu$ M. PG65 existed as predominantly monomeric when compared to other protein probes.  $\alpha$ S monomers ( $\alpha$ S M) were also run in the same native-PAGE gel for comparison. Numbers indicate positions of various molecular weight standard proteins. Note that migration of a protein in a native-PAGE gel depends not only on molecular weight, but also charge and conformation of the protein, and thus accurate molecular weight determination of a protein using native-PAGE is difficult. (B) SEC spectra of PG65 at 35  $\mu$ M (red line),  $\alpha$ S monomer ( $\alpha$ S M) sample at 35  $\mu$ M (blue line), a mixture of PG65 +  $\alpha$ S M sample at 35  $\mu$ M each (green line) and a simple sum of individual spectra of PG65 and  $\alpha$ S M sample (black line). PG65 remained mostly monomeric in aqueous buffer for > 3 hours under this condition. Elution times of the major peaks were the same in all samples and the ratio of the major peak area of the mixture sample (i.e., PG65 +  $\alpha$ S M sample) to that of the simple sum of individual proteins was  $1.01 \pm 0.03$ , indicating the lack of strong binding between PG65 and  $\alpha$ S monomers. The void volume for the SEC column corresponded to 10 min under our experimental setup. (C) A CD spectra illustrating the intrinsically disordered nature of PG65.

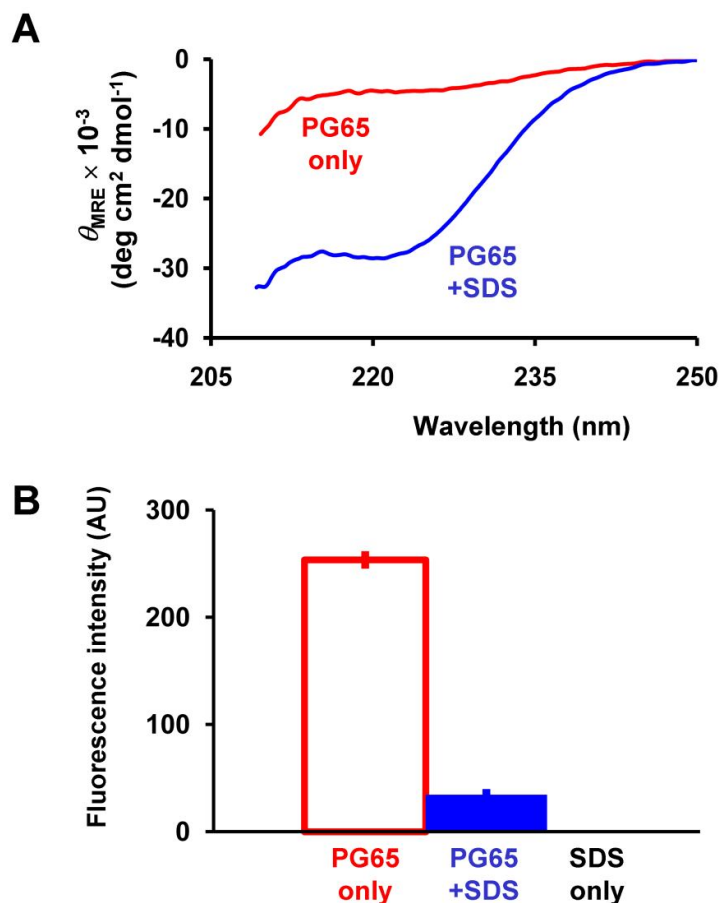


Fig. S3 (A) CD spectra of PG65 in the presence (blue line) and absence (red line) of 0.75 mM SDS. (B) FAsH fluorescence of PG65 in the presence (blue filled bar) and absence (red empty bar) of 0.75 mM SDS. Results shown in (A) and (B) illustrate that PG65 was structurally flexible, displaying an SDS-dependent structural change similar to  $\alpha S^1$  and this structure change was linked to FAsH fluorescence change. The implication is that PG65 generated FAsH fluorescence signals in its conformation-dependent manner. There was no significant change in CD and FAsH fluorescence signals of PG65 in the presence of 0.1 mM SDS when compared to a PG65 only control (data not shown).

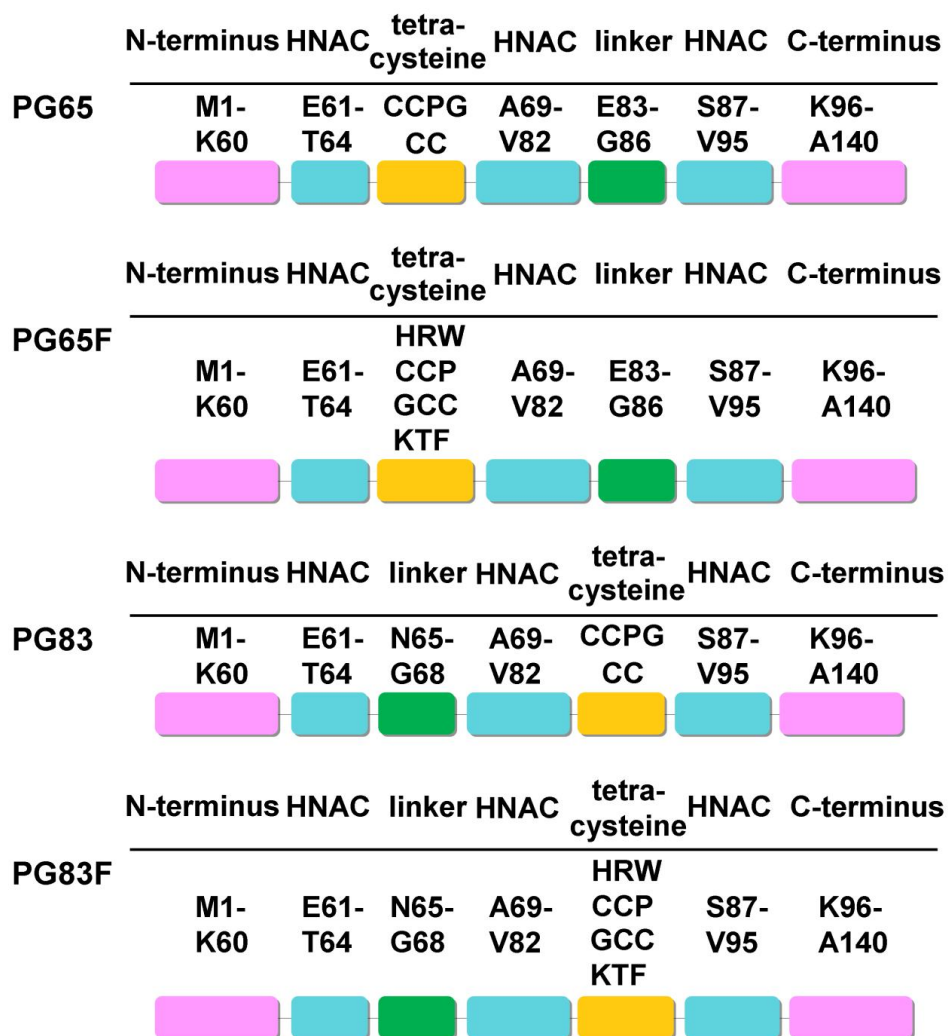


Fig. S4 Amino acid sequence schematics of PG65, PG65F, PG83 and PG83F. The sequences of PG65 and PG83 are similar to that of  $\alpha$ S, except for replacement of the first or second linker region, respectively, with CCPGCC. PG65F and PG83F are similar to PG65 and PG83, respectively, except for the addition of HRW and KTF residues flanking CCPGCC. Inclusion of additional flanking residues HRW and KTF to the ends of a tetracysteine motif was previously found to improve FIAsh fluorescence.<sup>2</sup>

## Characterization of $\alpha$ S samples: monomeric, oligomeric and fibrillar species prepared *in vitro*

We characterized molecular and morphological properties of  $\alpha$ S aggregate species that we prepared and isolated *in vitro* (see “ $\alpha$ S sample preparation” in Experimental Details for preparation of  $\alpha$ S monomer ( $\alpha$ S M),  $\alpha$ S oligomer ( $\alpha$ S O) and  $\alpha$ S fibril samples ( $\alpha$ S F)), and compared with results from similar previous characterization. Overall, our  $\alpha$ S monomer,  $\alpha$ S oligomer and  $\alpha$ S fibril samples exhibited distinct molecular and morphological properties, which were in agreement with those previously reported elsewhere.<sup>3,4</sup>

$\alpha$ S monomer ( $\alpha$ S M) samples we prepared displayed no significant fluorescence when mixed with thioflavin T (ThT, Fig. S5C), a fluorescent dye specific for cross  $\beta$  sheet structures present in amyloid fibrils.<sup>5</sup> No immuno-specific signal was detected when these  $\alpha$ S monomer samples were probed with A11 (Fig. S5D), an antibody known to recognize certain conformations of amyloid oligomers, including  $\alpha$ S oligomers.<sup>3,6</sup> Solvent-exposed hydrophobicity of  $\alpha$ S in these samples was low as determined by fluorescence of 1-anilinonaphthalene-8-sulfonic acid (ANS) (Fig. S5E), a fluorescent marker for exposed hydrophobic patches.<sup>7</sup> In these  $\alpha$ S samples, structurally disordered monomeric  $\alpha$ S represented the dominant fraction as determined by native-PAGE and CD analyses (Figs. S5A and B), while the presence of low molecular weight (LMW) oligomeric  $\alpha$ S was also detected in a native-PAGE gel (Fig. S5A) and TEM images (Fig. S5F), as described previously.<sup>3,4</sup> Additional separation of LMW  $\alpha$ S oligomers from  $\alpha$ S monomer samples was not performed. Note that LMW  $\alpha$ S oligomers were present in  $\alpha$ S solutions freshly prepared at room temperature without any incubation at 37 °C (Fig S5A).

Our  $\alpha$ S oligomer ( $\alpha$ S O) samples contained  $\alpha$ S species referred to in this study as high molecular weight (HMW) oligomeric  $\alpha$ S, which migrated more slowly than LMW  $\alpha$ S oligomers and  $\alpha$ S monomers in native-PAGE (Fig. S5A) and were mostly  $\beta$  sheet-structured. (Fig. S5B). Similar electrophoretic patterns of  $\alpha$ S monomers, and LMW and HMW  $\alpha$ S oligomers were reported in a previous native-PAGE analysis.<sup>3,4</sup> No significant ThT fluorescence was observed with our  $\alpha$ S oligomer samples, indicating the lack of  $\alpha$ S fibrillar structures in these samples (Fig. S5C). These  $\alpha$ S oligomer samples were significantly ANS-fluorescent (Fig. S5E) and A11-positive (Fig. S5D), indicating the existence of solvent-exposed hydrophobic patches and specific amyloid oligomer conformations, consistent with previous findings.<sup>3,4</sup> The predominant presence of spheroidal and “donut-like” annular oligomers with sizes in the range of 10-40 nm (Fig. S5F, inset) was detected in these  $\alpha$ S oligomer samples by transmission electron microscopy (TEM).  $\alpha$ S oligomers we prepared seeded  $\alpha$ S fibrillization as determined by ThT fluorescence (Fig. S6), consistent with the notion that these  $\alpha$ S oligomers may be intermediates on the  $\alpha$ S fibrillization pathway. Collectively, our  $\alpha$ S oligomers isolated after 6 hr incubation of freshly prepared  $\alpha$ S solutions followed by ultrafiltration displayed molecular and morphological characteristics similar to other  $\alpha$ S oligomers prepared by different means (see Table S1), including those shown to be cytotoxic,<sup>4,8,9</sup> indicative of the biological relevance of our  $\alpha$ S oligomer samples.

$\alpha$ S fibrillar ( $\alpha$ S F) samples that we prepared displayed a much higher ThT fluorescence signal when compared to  $\alpha$ S monomers and  $\alpha$ S oligomers (Fig. S5C). Our  $\alpha$ S fibril samples exhibited significant ANS fluorescence (Fig. S5E) and were A11-negative (Fig. S5D), as reported similarly elsewhere.<sup>3,4,6,10</sup> TEM images confirmed the presence of mature fibrils in these samples (Fig. S5F).

Isolation of  $\alpha$ S aggregate species, particularly  $\alpha$ S oligomers, was necessary to accurately determine detection specificity and sensitivity of our molecular probes (e.g., PG65) because the mass fraction of  $\alpha$ S oligomers was found to be very low (~5-20%) at all times during  $\alpha$ S aggregation, in agreement with previous reports.<sup>8,9,11-13</sup> In the present study, we first evaluated detection specificity and sensitivity of PG65 using pre-formed, isolated samples of  $\alpha$ S monomers ( $\alpha$ S M),  $\alpha$ S oligomers ( $\alpha$ S O) and  $\alpha$ S fibrils ( $\alpha$ S F). We then performed additional evaluation of PG65 with  $\alpha$ S solution withdrawn at various time points, without any additional separation, during long-term incubation under the same condition used to produce our  $\alpha$ S O and  $\alpha$ S F samples.

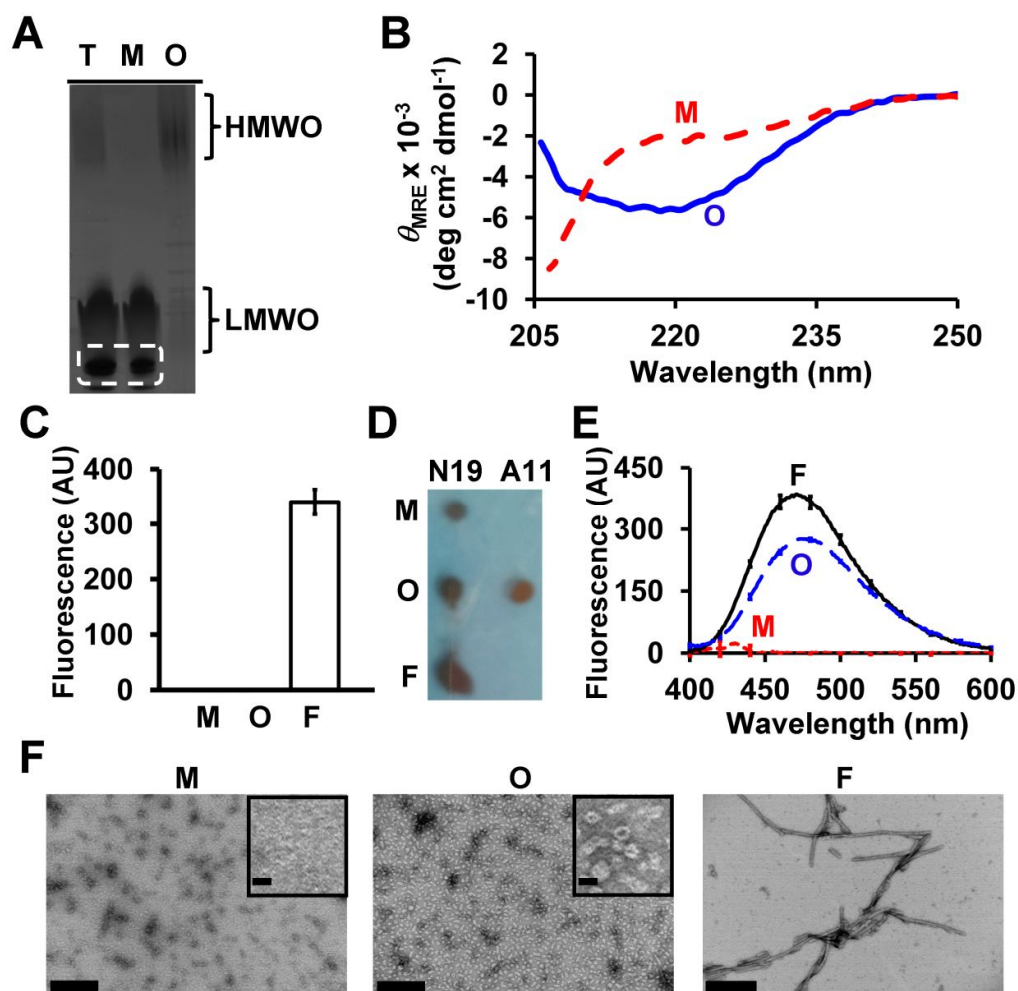


Fig. S5 (A) Native-PAGE of freshly prepared  $\alpha$ S sample (T),  $\alpha$ S monomer sample (M) and  $\alpha$ S oligomer sample (O) containing HMW  $\alpha$ S oligomer species (HMWO). See “ $\alpha$ S sample preparation” in Experimental Details for preparation of  $\alpha$ S M and  $\alpha$ S O samples. The bands corresponding to  $\alpha$ S monomeric states are shown in the white enclosed dashed line. The presence of LMW  $\alpha$ S oligomeric species (LMWO) in  $\alpha$ S M and  $\alpha$ S O samples was also detected and no further separation was attempted. (B) CD spectra of  $\alpha$ S monomer (M, red dotted line) and  $\alpha$ S oligomer samples (O, blue solid line). (C) Thioflavin T (ThT) fluorescence, (D) A11 dot blot assays, (E) ANS fluorescence and (F) transmission electron microscopy (TEM) images of  $\alpha$ S monomer (M),  $\alpha$ S oligomer (O) and  $\alpha$ S fibril (F) samples we prepared. See “ $\alpha$ S sample preparation” in Experimental Details for preparation of  $\alpha$ S M,  $\alpha$ S O and  $\alpha$ S F samples. In (D), 1  $\mu$ g of  $\alpha$ S from  $\alpha$ S M,  $\alpha$ S O, or  $\alpha$ S F samples was dotted onto a nitrocellulose membrane and probed with A11 and N19. A11 recognizes specific conformational structures present in certain oligomers formed by various amyloidogenic proteins<sup>6</sup>. N19 is a sequence specific antibody recognizing the N-terminus of  $\alpha$ S.<sup>14</sup> In (F), insets represent 5x magnification, highlighting the morphological differences between  $\alpha$ S species present in  $\alpha$ S monomer and  $\alpha$ S oligomer samples. The inset image of  $\alpha$ S oligomer samples illustrates annular and donut-like morphology of  $\alpha$ S aggregates. Scale bars represent 200 nm in larger images. Inset scale bars represent 20 nm.



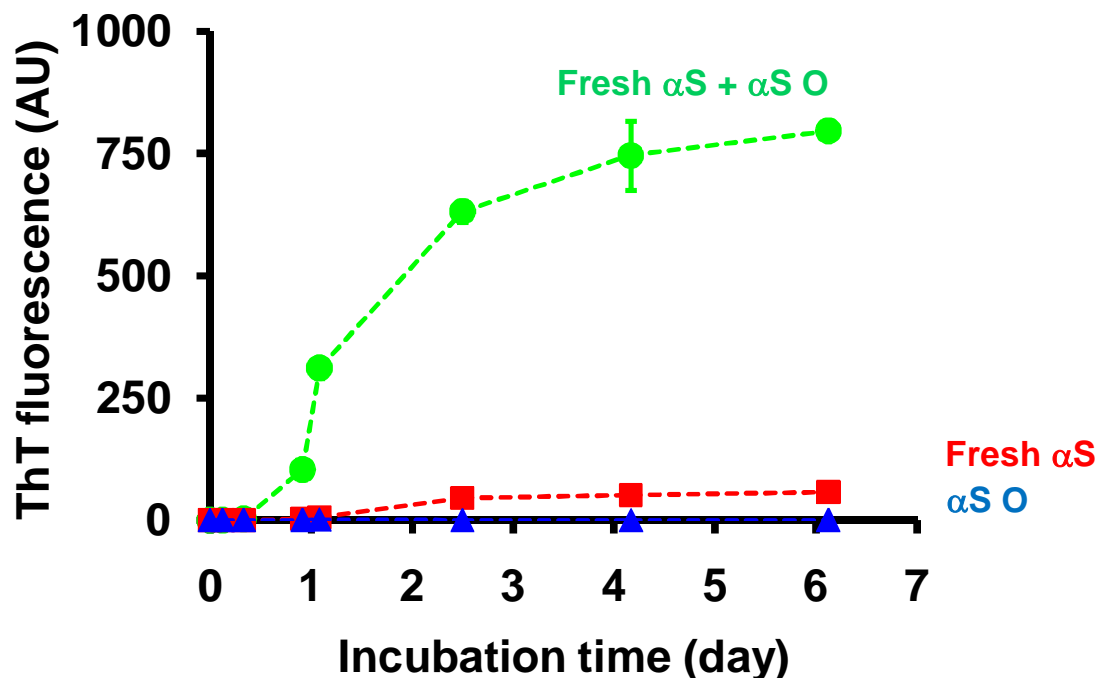


Fig. S6 Time-course aggregation monitored by ThT fluorescence during long-term incubation at 37 °C under a constant orbital shaking condition of a freshly prepared  $\alpha$ S solution at 350  $\mu$ M (red squares), a pre-formed  $\alpha$ S oligomer solution ( $\alpha$ S O), mostly HMW, at 30  $\mu$ M (blue triangles) and a mixture solution of freshly prepared  $\alpha$ S at 320  $\mu$ M +  $\alpha$ S oligomer ( $\alpha$ S O), mostly HMW, at 30  $\mu$ M (green circles). Concentrations are monomer-equivalent molar concentrations. Aliquots of samples were taken at several time points during incubation, then mixed with ThT prior to immediate ThT fluorescence measurements. See “ $\alpha$ S sample preparation” in Experimental Details for preparation of  $\alpha$ S oligomer ( $\alpha$ S O) samples. Results shown here indicate that the presence of HMW  $\alpha$ S oligomers shortened a lag-phase of  $\alpha$ S aggregation and accelerated  $\alpha$ S fibrillization. In other words, HMW  $\alpha$ S oligomers we prepared seeded  $\alpha$ S fibrillization, consistent with the notion that these  $\alpha$ S oligomers are on the fibrillization pathway.

Table S1. Molecular and morphological characteristics of  $\alpha$ S oligomer samples previously reported elsewhere in comparison with those prepared in this study

Mode of production (isolated vs. non-isolated <sup>a</sup> )	A11 response	Secondary structure	Electrophoretic pattern in native-PAGE	Morphology (method <sup>b</sup> and size)	ThT fluorescence	Seeding $\alpha$ S fibrilization	Toxicity	On-fibrilization pathway	Reference
SEC-isolated	Positive	$\beta$ sheet	Migrating more slowly than $\alpha$ S monomers	Spheroidal/donut-like (TEM, size: ~10 nm)	ND	ND	Toxic	ND	4
SEC-isolated	ND	$\beta$ sheet	ND	ND	ND	ND	Toxic	Yes	8
Ultrafiltration-isolated	Positive	$\beta$ sheet	Migrating more slowly than $\alpha$ S monomers	Spheroidal/donut-like (TEM, size: ~10-60 nm)	Little or no	Yes	ND	Yes	3
Non-isolated	Positive	$\beta$ sheet	Migrating more slowly than $\alpha$ S monomers	Spheroidal (TEM, size: ~10-30 nm)	Little or no	ND	ND	Yes	13
Non-isolated	ND	ND	ND	Spheroidal/donut-like (Small angle X-ray scattering and modeling, size: ~10-20 nm)	Little or no	ND	ND	Yes	11
Non-isolated	ND	$\beta$ sheet	ND	ND	ND	ND	Toxic	Yes	9
Ultrafiltration-isolated <sup>c</sup>	Positive	$\beta$ sheet	Migrating more slowly than $\alpha$ S monomers	Spheroidal/donut-like (TEM, size: ~10-40 nm)	Little or no	Yes	ND	Yes	In this study

<sup>a</sup>Samples were characterized either after isolation of  $\alpha$ S oligomers or without any separation

<sup>b</sup>In contrast with solution-based analysis, TEM analysis requires surface binding of  $\alpha$ S species and may be influenced by their surface contacts.

<sup>c</sup>See “ $\alpha$ S sample preparation” in Experimental Details for preparation of  $\alpha$ S oligomer ( $\alpha$ S O) samples. ND: not determined



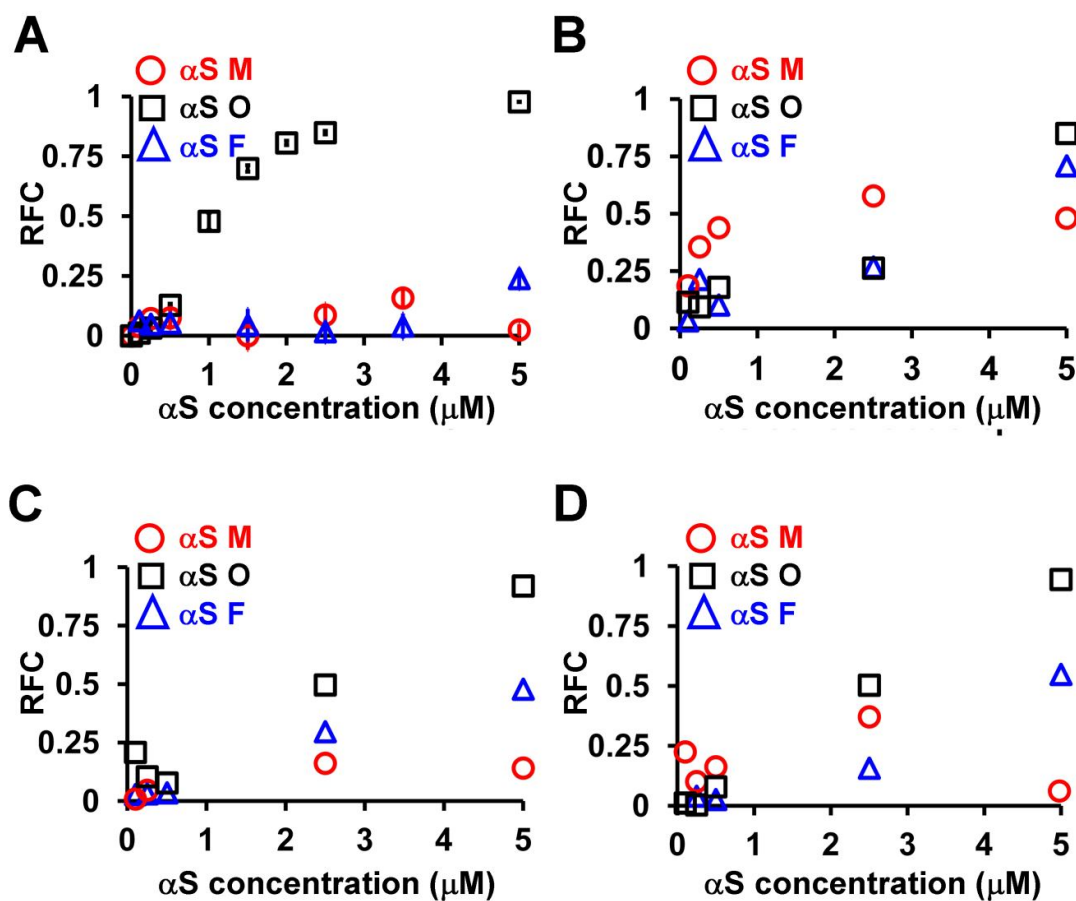


Fig. S7 Relative FIASH fluorescence changes (RFCs) of (A) PG65, (B) PG65F, (C) PG83 and (D) PG83F at 0.5  $\mu$ M as a function of concentrations of  $\alpha$ S monomer samples ( $\alpha$ S M, red circles),  $\alpha$ S oligomer samples ( $\alpha$ S O, black squares) and  $\alpha$ S fibril samples ( $\alpha$ S F, blue triangles). In A-D, samples containing pre-formed, isolated  $\alpha$ S monomers ( $\alpha$ S M),  $\alpha$ S oligomers ( $\alpha$ S O) or  $\alpha$ S fibrils ( $\alpha$ S F) at a designated concentration were mixed with the designated probe freshly prepared at 0.5  $\mu$ M followed by the addition of FIASH at 1.5  $\mu$ M. See “ $\alpha$ S sample preparation” in Experimental Details for preparation of  $\alpha$ S M,  $\alpha$ S O and  $\alpha$ S F samples. Concentrations of PG65, PG65F, PG83, PG83F and  $\alpha$ S are monomer-equivalent molar concentrations.

## Binding between PG65 and $\alpha$ S

We examined binding between PG65 and  $\alpha$ S using native-PAGE and its relevance to FIAsh fluorescence signaling. For specific identification of  $\alpha$ S and PG65, we labeled them with Alexa Fluor 488 and Alexa Fluor 647 at their respective N-terminus. Note that similar N-terminal labeling did not affect self-assembly properties of  $\alpha$ S and  $\alpha$ S linker mutants.<sup>12</sup> The location of the major PG65 bands corresponding to the size of PG65 monomers remained unchanged in the presence of  $\alpha$ S monomers (Fig. S8A), indicating the lack of significant binding between these two entities, which was further confirmed by relevant SEC analysis (Fig. S2B). The lack of such binding may be due to a high thermodynamic cost of assembly between structurally disordered protein forms and appears to cause no resulting fluorescence signaling (Fig. 1B). Additional minor bands of PG65 also appeared as a result of its binding to LMW  $\alpha$ S oligomers present as the small fraction in  $\alpha$ S monomer ( $\alpha$ S M) samples (Figs. S8A and S5A). While similar minor bands of PG65 were also apparent for a mixture of PG65 and  $\alpha$ S oligomer ( $\alpha$ S O) samples (Fig. S8B), we also observed new overlapping bands in this mixture, an indication of binding between HMW  $\alpha$ S oligomers and PG65 (Fig. S8B). Moreover, comparison between Fig. 1B and Figs. S8A-B suggests that these new overlapping bands represented the molecular binding event, which triggered generation of FIAsh fluorescence signals. We then isolated PG65 bound to HMW  $\alpha$ S oligomers and FIAsh after removing free PG65 and free FIAsh using ultrafiltration and measured the quantum yield of this complex with assumption that all PG65 molecules were bound to FIAsh. FIAsh bound to PG65 without  $\alpha$ S was also prepared as a control after removing unbound FIAsh using ultrafiltration. The quantum yields of FIAsh in these two cases differed by  $\sim 9$ -fold, which was consistent with the observed RFCs of PG65 with  $\alpha$ S oligomer ( $\alpha$ S O) samples (Fig. 1B).

Binding of PG65 to  $\alpha$ S was further examined by fluorescence dot blot assays where  $\alpha$ S monomer ( $\alpha$ S M),  $\alpha$ S oligomer ( $\alpha$ S O) and  $\alpha$ S fibril ( $\alpha$ S F) samples were blotted onto nitrocellulose membranes, probed by Alexa Fluor 647-labeled PG65 and then imaged using fluorescence (Fig. S8C). To minimize any complication associated with formation of disulfide bonds between PG65 and blocking proteins in a dot blot assay, we mutated all cysteines of Alexa 647-labeled PG65 to serines.  $\alpha$ S O samples at 10  $\mu$ g displayed positive signals in this format, further confirming the existence of the molecular binding event between PG65 and  $\alpha$ S oligomers as characterized by native-PAGE (Fig. S8B). Fluorescent dot blot signals were rarely detected with  $\alpha$ S O samples at 1  $\mu$ g (Fig. S8C).  $\alpha$ S M samples at 1 – 10  $\mu$ g were positive in this assay (Fig. S8C). These results, together with those obtained from native-PAGE analyses (Figs. S8A-B), support that PG65 was bound to LMW  $\alpha$ S oligomers present in the  $\alpha$ S M samples presumably more strongly than HMW  $\alpha$ S oligomers. Similar positive fluorescent dot blot signals were observed with  $\alpha$ S F samples at 1 – 10  $\mu$ g, indicating that PG65 was bound to  $\alpha$ S fibrils with no weaker affinity than to  $\alpha$ S HMW oligomers (Fig. S8C). Together with Fig. 1B, our binding results suggest that generation of PG65 fluorescence signals did not simply depend on binding events, but also on aggregation states of bound  $\alpha$ S.

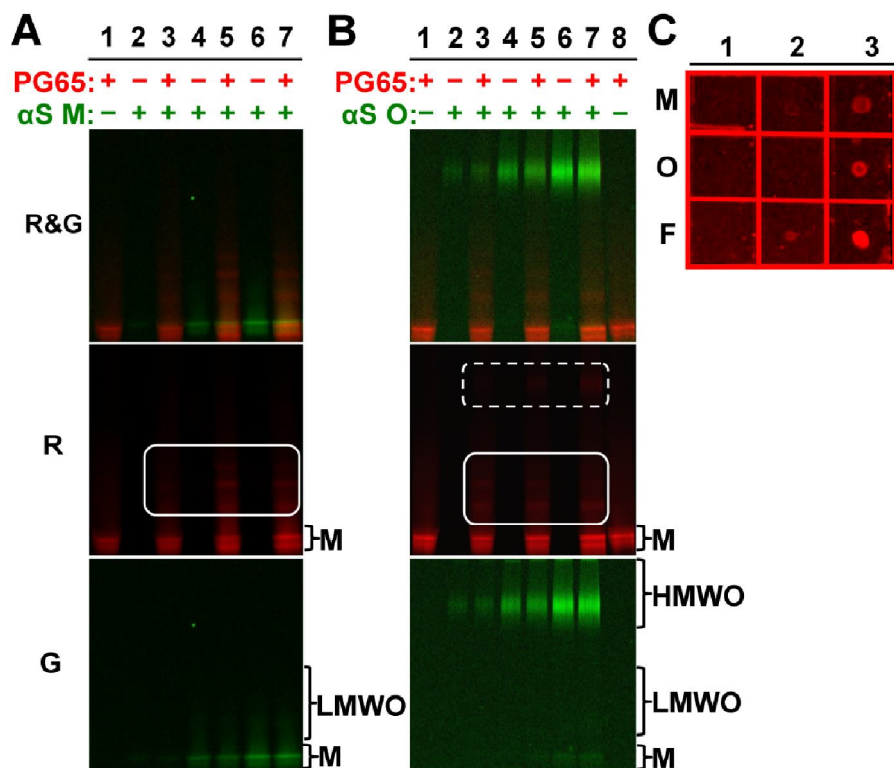


Fig. S8 (A-B). Native-PAGE of PG65 (red, R), αS (green, G), and a mixture of PG65 (red, R) + αS (green, G) at different molar concentrations of αS in (A) αS monomer (αS M) and (B) αS oligomer (αS O) samples. PG65 and αS were labeled with fluorescent dyes, Alexa Fluor 647 and Alexa Fluor 488, respectively. Concentration of PG65: 3.4 μM (lanes 1, 3, 5, 7 and 8) and concentration of αS: 2.5 μM (lanes 2 and 3), 10 μM (lanes 4 and 5), 20 μM (lanes 6 and 7). PG65 at < 3.4 μM was not used because of insufficient fluorescence emission for imaging. (A-B). Additional bands of PG65 formed as a result of its binding to LMW αS oligomers and HMW αS oligomers are shown in the enclosed solid and dashed lines, respectively. M: monomeric state, LMWO: LMW αS oligomers and HMWO: HMW αS oligomers. (C). Fluorescent dot blot assays of αS monomer (M), αS oligomer (O) and αS fibril (F) samples at 0.1 (column 1), 1 (column 2) and 10 μg (column 3) of αS probed with Alexa Fluor 647-labeled PG65 containing Cys to Ser mutations. In A-C, PG65 solution was freshly prepared each time and mixed with pre-formed αS M, αS O or αS F samples. See “αS sample preparation” in Experimental Details for preparation of αS M, αS O and αS F samples.

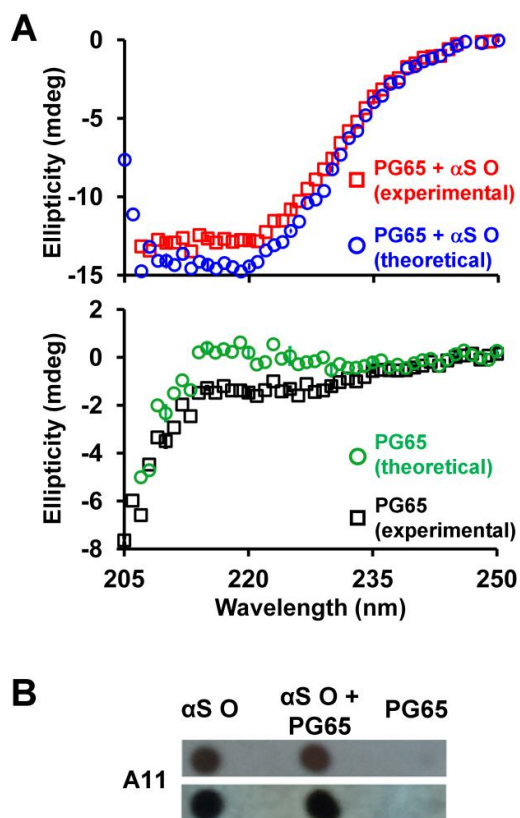


Fig. S9 (A) Top: A CD spectrum of a mixture of PG65 +  $\alpha$ S oligomer ( $\alpha$ S O) sample (red squares) shown along with their corresponding theoretical mixture (i.e., the simple sum of the individual spectra for PG65 only and  $\alpha$ S O sample only under the otherwise same conditions, blue circles). Bottom: To draw structural information of PG65 bound to  $\alpha$ S O, we subtracted the CD spectrum of  $\alpha$ S O only sample from that of a mixture of PG65 +  $\alpha$ S O sample (the resulting spectrum shown as green circles). We then compared the resulting CD spectrum with the CD spectrum of PG65 only (black squares). As described in the main text, a difference between these two CD spectra (i.e., PG65 theoretical and PG65 experimental) is likely to be related to structural changes occurring in PG65 rather than  $\alpha$ S O upon binding to each other. The comparison of these two CD spectra shows a gain of broad positive ellipticity at  $\sim$ 215-225 nm upon mixing of PG65 with  $\alpha$ S O, suggesting formation of local, not necessarily global, residual poly(Pro)II helical structures in PG65 upon binding to  $\alpha$ S O. The presence of similar residual poly(Pro)II helical structures was found in other proteins at structurally disordered states.<sup>15-17</sup> Poly(Pro) II helical structures can be formed by even a single peptide bond<sup>16</sup>, and similar helical structures are found in poly(Gly)<sup>18</sup>, raising a possibility that Pro-Gly within the signal domain of PG65 adopt poly(Pro)II-like helical structures. The implication, together with other results described in the current study, is that binding to  $\alpha$ S oligomers might cause structural changes of PG65 to poly(Pro)II-like helical structures, possibly locally in the signal domain (e.g., Pro-Gly), but not necessarily globally, and this conformational change could induce relative FLAsH fluorescence changes (RFCs). Top and Bottom: Concentration of PG65: 2.6  $\mu$ M and concentration of  $\alpha$ S: 13  $\mu$ M. Error bars (i.e., 1 SD) are included at every 5 nm and smaller than data symbols. PG65 at < 2.6  $\mu$ M was not used because of low signal-to-noise ratios of CD signals under this condition. No significant difference in CD spectra of protein samples was detected in the presence and absence of an excess of FLAsH (data not shown). (B) Dot blot assays of  $\alpha$ S oligomer ( $\alpha$ S O) samples with and without PG65 using a conformation-specific antibody, A11. [ $\alpha$ S O]/[PG65] = 1:1 (top) and 5:1 (bottom). In A-B, PG65 solution was freshly prepared each time and mixed with pre-formed  $\alpha$ S O samples. See “ $\alpha$ S sample preparation” in Experimental Details for preparation of  $\alpha$ S O samples.

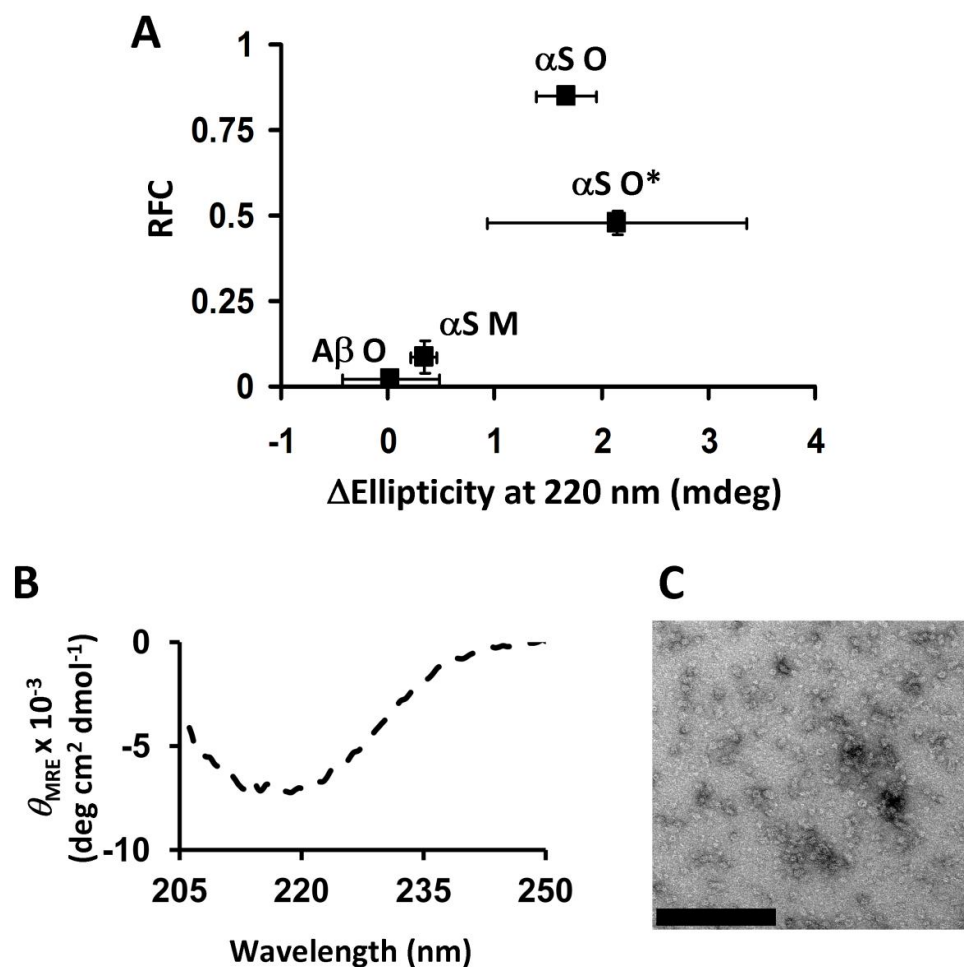


Fig. S10 (A) Relative FIAsh fluorescence change (RFC) is compared against the ellipticity difference at 220 nm between actual and theoretical mixtures of PG65 at 2.6  $\mu$ M with  $\alpha$ S monomers ( $\alpha$ S M),  $\alpha$ S oligomers prepared after 0 hr incubation ( $\alpha$ S O\*, see Figs. S10B and C for characterization of  $\alpha$ S O\* samples),  $\alpha$ S oligomers prepared after 6 hr incubation ( $\alpha$ S O) and A $\beta$  oligomer samples (A $\beta$  O) each at 13  $\mu$ M. See “ $\alpha$ S sample preparation” in Experimental Details for preparation of  $\alpha$ S M,  $\alpha$ S O\* and  $\alpha$ S O samples. A $\beta$  O samples were prepared as described in our previous study<sup>19</sup> (also see “A $\beta$  sample preparation” in Experimental Details) and were A11-positive,  $\beta$  sheet-structured, ThT-positive and protofibrillar.<sup>19</sup> For RFC measurements, PG65 solution was freshly prepared at 0.5  $\mu$ M and mixed with pre-formed  $\alpha$ S M,  $\alpha$ S O\*,  $\alpha$ S O and A $\beta$  O samples at 2.5  $\mu$ M each, followed by the addition of 1.5  $\mu$ M of FIAsh for fluorescence measurements. The errors were evaluated using the propagation of error method. Fig. S10A suggests that secondary structure change of PG65 might be necessary to yield significant RFC. (B-C) Characterization of  $\alpha$ S O\* oligomer samples.  $\alpha$ S O\* oligomers displayed (B)  $\beta$  sheet-structures and (C) non-fibrillar morphology.  $\alpha$ S O\* oligomers were A11-positive and ThT-negative (data not shown). The scale bar in (C) represents 200 nm.

### Limitation of the use of PG65

For quantitative measurements of  $\alpha$ S oligomers present in an unknown sample, a standard curve (e.g., data shown in Fig. 1) should first be prepared where RFCs of PG65 are measured at different concentrations of  $\alpha$ S oligomers under a condition similar to that used for preparation of the unknown sample. Using the standard curve, one can quantify the amount of  $\alpha$ S oligomers present in an unknown sample by measuring RFC of PG65 with the sample. Detection of  $\alpha$ S oligomers using PG65 was not compromised by the presence of  $\alpha$ S monomers and  $\alpha$ S fibrils, as described in the main text, increasing the likelihood of  $\alpha$ S synuclein oligomer detection in an unknown sample containing other  $\alpha$ S species (i.e., monomers and fibrils). Also, note that a highly reliable quantification of  $\alpha$ S oligomers present in biological samples may be achieved if a standard curve is generated with biologically-relevant or biologically-derived  $\alpha$ S oligomers. Moreover, thorough and comprehensive testing of PG65 under a complex and biologically-relevant setup will be required for applications of PG65 for  $\alpha$ S oligomer detection in biological samples, where significant complexity and nonspecific interactions exist under highly crowded conditions. While one may use PG65 for fluorescence-based high-throughput assays to identify molecular agents specifically inhibiting  $\alpha$ S oligomerization, several limitations are realized for  $\alpha$ S oligomer detection using PG65. For example, detection of  $\alpha$ S oligomers using PG65 is currently limited to an *in vitro* use. While fluorescence of FLAsH and its derivatives has been successfully applied for imaging proteins at various cellular locations in single cells as well as tissues<sup>20, 21</sup>, applications of PG65 for *in vivo* diagnostics requires additional examinations, such as those on its toxicity, membrane permeability, delivery across the blood brain barrier and aggregation propensity *in vivo*.



## Experimental Details

### *Reagents*

Oligonucleotides were purchased from Operon Biotechnologies Inc. (Huntsville, AL, USA). High-fidelity Platinum Pfx DNA polymerase and BL21(DE) cells were purchased from Life Technologies (Grand Island, NY, USA). All DNA purification kits were purchased from Qiagen (Valencia, CA, USA). FPLC columns for purification were purchased from GE Healthcare (Rahway, NJ, USA). Restriction enzymes and T4 DNA ligase were purchased from New England Biolabs (Ipswich, MA, USA). Antibiotics and biological reagents were purchased from Thermo Fisher Scientific (Suwanee, GA, USA). Antibodies recognizing the N and C-terminus of  $\alpha$ S were purchased from Santa Cruz Biotechnologies (Santa Cruz, CA, USA). A conformation-specific antibody, A11, was purchased from Life Technologies (Grand Island, NY, USA).

### *DNA construction*

The plasmid pRK172<sup>22-24</sup> was used for expression of  $\alpha$ S, PG65, PG65F, PG83 and PG83F. DNA sequences coding for protein probes were created by overlap extension PCR. The desired PCR products were purified by QIAquick PCR purification and QIAquick gel-extraction kits. The purified DNA sequences were digested by NdeI and HindIII restriction enzymes to create the sticky ends needed for ligation. Plasmid pRK172 was digested with the same enzymes, and purified with a QIAquick gel-extraction kit. The digested inserts and plasmids were then ligated using T4 ligase. Ligation products were then electroporated into 90  $\mu$ L of BL21(DE3) using a Bio-Rad Gene Pulser (Hercules, CA, USA). Electroporated cells were subsequently incubated for 1 hr at 250 rpm and 37 °C in a New Brunswick Scientific Innova TM4230 incubator (Edison, NJ, USA). Electroporated cells were then plated on an LB agar plate supplemented with 100  $\mu$ g/mL of ampicillin and incubated for 16–24 hr at 37 °C in the incubator. The colonies growing on the ampicillin-supplemented LB agar plate were picked and re-cultured in test tubes containing 10 mL of LB medium and 100  $\mu$ g/mL of ampicillin. Plasmid DNA was extracted from re-cultured colonies by using a QIAprep spin miniprep kit according to the manufacturer's protocol. The extracted DNA was then sequenced at Genewiz, Inc. (South Plainfield, NJ, USA). Cysteine to serine mutations were introduced into a gene encoding PG65 by Quikchange mutagenesis (Agilent Technologies, Santa Clara, CA, USA) and confirmed by DNA sequencing.

### *Protein expression and purification*

One liter of LB medium containing 50  $\mu$ g/mL of ampicillin was inoculated with 1 % overnight culture and shaken at 250 rpm and 37 °C. Cells expressing  $\alpha$ S and protein probes were grown at 37 °C until the OD<sub>600</sub> reached 1.0. Expression of  $\alpha$ S and protein probes was then induced by adding isopropyl- $\beta$ -D-1-galactopyranoside (IPTG) at 1 mM. After induction, the cell culture was shaken for another 18–20 hr at 250 rpm and 25 °C to express the proteins. Cells were pelleted by centrifugation at 4400g and 4 °C for 20 min in a Beckman Coulter Avanti JE centrifuge (Fullerton, CA, USA). The pelleted cells were then stored at -80 °C until use.

For protein purification, the pelleted cells were resuspended in Tris-HCl buffer (50 mM, pH 8.0) at a dilution ratio of approximately 10 mL per gram of cells. The cells were then lysed by sonication using a Branson Sonifier 150 (Danbury, CT, USA), and the cell lysates were centrifuged at 39000g and 4 °C for 1hr. Supernatants containing soluble proteins were then recovered and heat-treated at 80 °C, followed by another centrifugation at 39000g and 4 °C. Heat-treated supernatant was then passed through an anion-exchange column (HiTrap Q XL, GE Healthcare) where bound proteins (i.e.,  $\alpha$ S and probes) were eluted with NaCl (0.35 mM). Fractions containing proteins were then concentrated approximately ten-fold and run through a SEC column (HiPrep 16/60 Sephacryl S-100 High Resolution, GE Healthcare). Following SEC, proteins were desalted on a HiPrep 26/10 Desalting column (GE Healthcare), and eluted in deionized H<sub>2</sub>O. Purified  $\alpha$ S was then lyophilized and stored at -80 °C until use, and its identity was confirmed by MALDI-TOF mass spectrometry and dot blot



assays using antibodies that recognize the N- or C-terminus of  $\alpha$ S. Purification of protein probes followed a similar process, all in the presence of 1 mM TCEP to prevent formation of inter- and intra-molecular disulfide bonds of protein probes. After SEC, protein probe solutions were aliquoted and stored at -80 °C in the presence of 1 mM TCEP until use. The purities of the proteins were estimated by SDS-PAGE with Coomassie Blue staining to be greater than 95% (data not shown).

#### ***$\alpha$ S sample preparation***

For preparation of  $\alpha$ S monomer samples (referred to as  $\alpha$ S M samples in this paper), lyophilized  $\alpha$ S was solubilized at a concentration of ~350  $\mu$ M in phosphate buffered saline with azide (PBSA, 20 mM  $\text{Na}_2\text{HPO}_4/\text{NaH}_2\text{PO}_4$ , 150 mM NaCl, 0.02% (w/v)  $\text{NaN}_3$ , pH 7.2) at room temperature.  $\alpha$ S samples were then filtered at room temperature using 100 kDa cutoff Amicon Ultra centrifugal filters (Millipore, Billerica, MA, USA) with collection of the filtrate. Note that 100 kDa cutoff membranes were used for ultrafiltration to prepare monomeric  $\alpha$ S (MW: 14.5 kDa). This is because  $\alpha$ S monomers are natively unfolded and thus display the hydrodynamic size corresponding to that of ~60 kDa globular proteins.<sup>25-27</sup> Filtrates were used for subsequent characterizations without any additional separation.

For preparation of  $\alpha$ S oligomer samples (referred to as  $\alpha$ S O samples in this paper), lyophilized  $\alpha$ S was dissolved at ~420  $\mu$ M in PBSA at room temperature. Protein samples were filtered at room temperature with 0.45  $\mu$ m syringe filters into glass vials, and the concentrations of the filtered protein solutions were measured using the absorbance at 280 nm in 8 M urea.<sup>28</sup> The concentrations of filtered protein solutions in PBSA were immediately adjusted to 350  $\mu$ M by the addition of buffers at room temperature. Protein solutions were then subject to incubation at 37 °C under continuous orbital shaking conditions for 6 hr, followed by ultrafiltration through 100 kDa cutoff centrifugal filters with collection of the retentate at room temperature. Alternatively, freshly prepared  $\alpha$ S solution at 350  $\mu$ M was filtered using 100 kDa cutoff centrifugal filters without any incubation at 37 °C to prepare  $\alpha$ S oligomers after 0 hr incubation (referred to as  $\alpha$ S O\* samples in this paper).

$\alpha$ S fibril samples (referred to as  $\alpha$ S F samples in this paper) were prepared similar to the preparation of  $\alpha$ S O samples, except for prolonged incubation of  $\alpha$ S solution for ~2-3 weeks at 37 °C followed by centrifugation, multiple washing and rinsing with PBSA, and resuspension of the insoluble fraction in PBSA at room temperature.

Concentrations of  $\alpha$ S in this study are monomer-equivalent molar concentrations, unless otherwise mentioned.

#### ***$\beta$ amyloid (A $\beta$ ) sample preparation***

Oligomeric samples of A $\beta$  containing 42 amino acids (referred to as A $\beta$  O in this paper) were prepared as described in our previous study<sup>19</sup> where A $\beta$  lyophilized powders were pre-treated with hexafluoroisopropanol (HFIP) and then re-lyophilized. The HFIP-treated, re-lyophilized A $\beta$  was then solubilized at 400  $\mu$ M with 10 mM NaOH for 10 min. A $\beta$  solution in NaOH was then diluted into PBSA. The resulting A $\beta$  solution was incubated at 55  $\mu$ M and room temperature without any shaking. After 3 days of incubation, A $\beta$  soluble oligomers were separated from precipitates by centrifugation. These A $\beta$  oligomer samples contained protofibrils and displayed  $\beta$  sheet structures.<sup>19</sup> In these A $\beta$  oligomer samples, ~70 % of A $\beta$  molecules existed at oligomeric states with the remainder at monomeric states, as determined by SEC.<sup>19</sup> These A $\beta$  oligomer samples displayed ThT fluorescence, ~35 % of those intensities displayed by A $\beta$  fibrils.<sup>19</sup>

#### ***Measurement of FIAsh fluorescence of PG65***

Fresh aliquots of PG65 solutions at 50  $\mu$ M in PBSA containing 1 mM tris(2-carboxyethyl)phosphine (TCEP) was diluted 100-fold at room temperature into aqueous buffers containing  $\alpha$ S, 90  $\mu$ M TCEP and 100  $\mu$ M 1,2-ethanedithiol (EDT). The final concentration of PG65 after 100-fold dilution was 0.5

$\mu\text{M}$ . A similar dilution was made into the same buffers containing 90  $\mu\text{M}$  TCEP and 100  $\mu\text{M}$  EDT without  $\alpha\text{S}$  as a control. As another control, PBSA containing 1 mM TCEP was diluted 100-fold into  $\alpha\text{S}$  solutions containing 90  $\mu\text{M}$  TCEP and 100  $\mu\text{M}$  EDT. The final concentrations of TCEP and EDT were kept at 100  $\mu\text{M}$ , in all samples (i.e., PG65 only,  $\alpha\text{S}$  only and a mixture of PG65 plus  $\alpha\text{S}$ ). Similar addition of competing thiols (e.g., TCEP and EDT) strongly favors binding of FIAsh to a continuous tetracysteine motif, such as one contained in PG65, relative to non-continuous multiple cysteines.<sup>29</sup> The presence of such competing thiols also prevented formation of intra- and inter-molecular disulfide bonds of PG65. The samples were incubated for 1 hr at room temperature to allow binding between PG65 and  $\alpha\text{S}$  to a sufficient extent. After the initial 1 hr incubation, 200  $\mu\text{M}$  of FIAsh-EDT<sub>2</sub> in DMSO was diluted 133-fold into samples of PG65 only,  $\alpha\text{S}$  only and a mixture of PG65 plus  $\alpha\text{S}$ . The final concentration of FIAsh was 1.5  $\mu\text{M}$ , unless otherwise mentioned. The samples were then further incubated for an additional 1 hr prior to FIAsh fluorescence measurements using a Photon Technology QuantaMaster QM-4 spectrofluorometer. The final volumes of samples in cuvettes for FIAsh fluorescence measurements were 150  $\mu\text{l}$ . The excitation wavelength was 508 nm and emission was monitored at 536 nm. The data obtained were used for calculation of relative FIAsh fluorescence changes (RFCs) as signals, i.e., the absolute value ratio of (FIAsh fluorescence emission intensity of a mixture of PG65 plus  $\alpha\text{S}$  – (FIAsh fluorescence emission intensity of PG65 only + FIAsh fluorescence emission intensity of  $\alpha\text{S}$  only)) / (FIAsh fluorescence emission intensity of PG65 only). As such, this ratio must be 0 when there is no FIAsh fluorescence change of PG65 in the presence of  $\alpha\text{S}$ . The errors were evaluated by the propagation of error method using data obtained from measurements of at least six samples (i.e.,  $\geq 2$  samples for PG65 only,  $\geq 2$  samples for  $\alpha\text{S}$  only and  $\geq 2$  samples for a mixture of PG65 plus  $\alpha\text{S}$ ). Concentrations of PG65 and  $\alpha\text{S}$  are monomer-equivalent molar concentrations. All samples were prepared in siliconized tubes. Significant RFCs were still observed when samples were incubated for 30 min in each step (1 hr total). For example, in the presence of  $\alpha\text{S}$  oligomers at 2.5  $\mu\text{M}$ , RFCs of PG65 at 0.5  $\mu\text{M}$  was measured to be 0.11, 0.15 and 0.65 after incubation for 10 min, 20 min and 30 min in each step (i.e., 20 min, 40 min and 1 hr total, respectively). These values corresponded to 12, 18 and 76 %, respectively, of the RFC value of PG65 with  $\alpha\text{S}$  oligomers at 2.5  $\mu\text{M}$  shown in Fig. 1 (i.e., after total 2 hr incubation), indicating that significant RFC occurred during the first 1 hr incubation and an additional RFC increase was marginal upon further incubation. During incubation with PG65, aggregation states of  $\alpha\text{S}$  (e.g., oligomeric) remained unchanged (Figs. S8A-B). Incubation of PG65 with  $\alpha\text{S}$  longer than 2 hr was not employed during detection because 1)  $\alpha\text{S}$  aggregation states may be potentially perturbed by PG65 in this case, as depicted in Fig. S11, at the cost of a marginal RFC increase and 2) relatively short incubation was much preferred for a rapid-responsive detection platform. Taken altogether, we reasoned that ~1-2 hr incubation is optimal for detection of  $\alpha\text{S}$  using PG65. PG65 at  $< 0.5 \mu\text{M}$  was not used in this study because of the relatively low signal-to-background ratio of FIAsh fluorescence. Concentrations of  $\alpha\text{S}$  we tested were 0 – 5  $\mu\text{M}$ . Higher concentrations of  $\alpha\text{S}$  were not tested due to the non-negligible background FIAsh fluorescence from  $\alpha\text{S}$  under this condition, particularly at the oligomeric and fibrillar states, presumably due to non-specific binding of FIAsh to solvent-exposed hydrophobic domains of  $\alpha\text{S}$  oligomers and  $\alpha\text{S}$  fibrils. RFCs of other protein probes (i.e., PG65F, PG83 and PG83F) with  $\alpha\text{S}$  were measured similarly.

Detection of  $\alpha\text{S}$  using FIAsh fluorescence of PG65 at 0.5  $\mu\text{M}$  was carried out with 1.5  $\mu\text{M}$  of FIAsh for maximal FIAsh fluorescence based on the following observations: when FIAsh fluorescence of PG65 at 0.5  $\mu\text{M}$  was measured with increasing concentrations of FIAsh, RFC values did not alter significantly with concentrations of FIAsh higher than 1.5  $\mu\text{M}$  in the presence and absence of  $\alpha\text{S}$  monomers,  $\alpha\text{S}$  oligomers, or  $\alpha\text{S}$  fibrils (data not shown), indicating that FIAsh is in excess under this condition. Additional incubation up to 6 hrs following addition of FIAsh yielded  $< 10\%$  variation in FIAsh fluorescence of PG65 in the presence and absence of  $\alpha\text{S}$ .

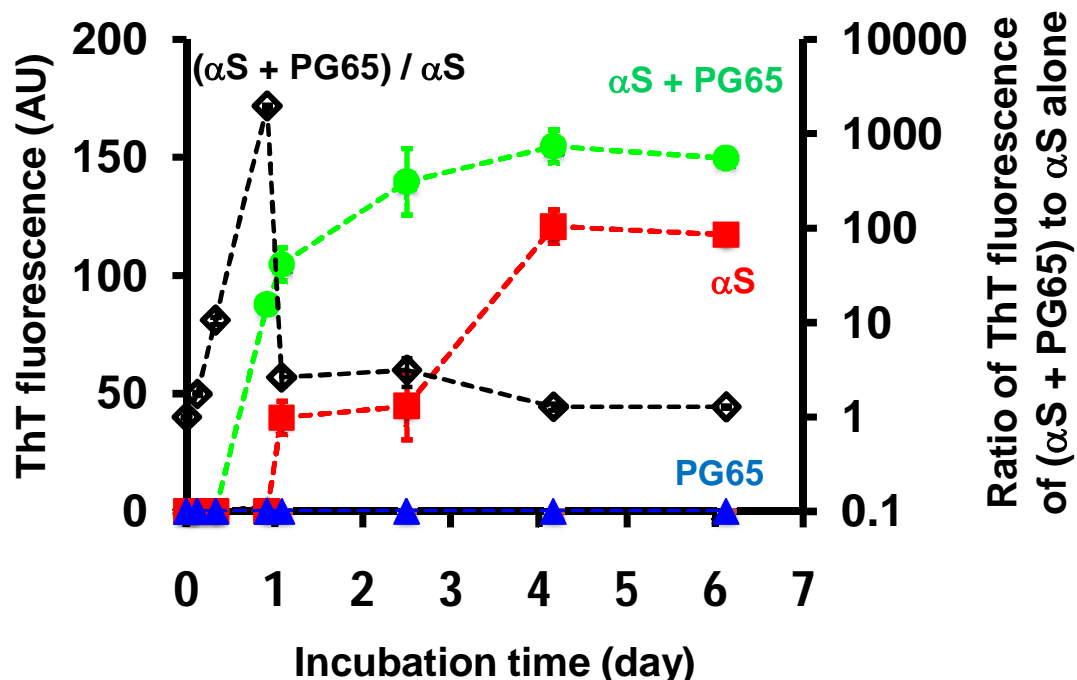


Fig. S11 Time-course aggregation monitored by ThT fluorescence during long-term incubation at 37 °C under a constant orbital shaking condition of a freshly prepared  $\alpha$ S solution at 350  $\mu$ M (red squares), a freshly prepared PG65 solution at 0.5  $\mu$ M (blue triangles) and a mixture solution of freshly prepared  $\alpha$ S at 350  $\mu$ M + freshly prepared PG65 at 0.5  $\mu$ M (green circles) presented in the primary Y-axis. Samples were aliquoted at several time points during incubation, then mixed with ThT prior to immediate ThT fluorescence measurements. Samples contained 100  $\mu$ M of TCEP to prevent formation of inter- and intra-molecular disulfide bonds of PG65. Errors are standard deviation of triplicate measurements. The data shown as empty black diamonds represent the ratio of ThT fluorescence of  $\alpha$ S + PG65 (i.e., green circles) to  $\alpha$ S alone (i.e., red squares) at a given time point and were presented in the secondary Y-axis. Time-course ThT fluorescence changes of  $\alpha$ S aggregation in the presence and absence of PG65 followed a typical sigmoidal curve as reported elsewhere.<sup>3, 30</sup> Results shown here indicate that the co-presence of PG65 accelerated  $\alpha$ S fibrillization upon long-term incubation. The lag-phase of  $\alpha$ S aggregation was shortened by the co-presence of PG65, suggesting that PG65 may promote formation of protein entities compatible with fibrillar aggregation. No significant self-aggregation of PG65 was detected under this condition.

The mixture containing fresh  $\alpha$ S at 350  $\mu$ M + fresh PG65 at 0.5  $\mu$ M was aliquoted after 6 hr incubation at 37 °C (i.e., prior to onset of a ThT fluorescence increase) and the aliquots were mixed with 1.5  $\mu$ M of FIAsh followed by FIAsh fluorescence measurements. As a control, solution of freshly prepared  $\alpha$ S alone at 350  $\mu$ M was aliquoted after 6 hr incubation at 37 °C and the aliquots were then mixed with freshly prepared PG65 at 0.5  $\mu$ M and FIAsh at 1.5  $\mu$ M followed by FIAsh fluorescence measurements. RFCs of PG65 in these two cases were similar (within  $\pm 10$  %), suggesting that the co-presence of PG65 in  $\alpha$ S solution might not affect formation of PG65-detectable  $\alpha$ S oligomers during incubation of freshly prepared  $\alpha$ S at 350  $\mu$ M and 37 °C for 6 hrs. Note that this result should not serve for exploration of PG65's therapeutic potentials, which could better be evaluated after comprehensive examination of its toxicity, membrane permeability, delivery across the blood brain barrier and aggregation propensity *in vivo*.

### ***Fluorescence labeling of $\alpha$ S and PG65***

Purified PG65 and  $\alpha$ S were labeled with highly photostable Alexa Fluor 647 and Alexa Fluor 488 (Life Technologies), respectively. Succinimidyl-ester forms of these dyes were mixed with purified proteins at pH 7.2 to promote N-terminal ( $\alpha$ -amine) labeling according to the manufacturer's protocol. For this labeling, the ratio of fluorescent dye to protein concentrations was adjusted to achieve a final labeling molar ratio of ~ 1:3–4. Alexa Fluor 488-labeled  $\alpha$ S was separated and collected from SEC on a HiPrep 16/60 Sephacryl S-100 column, desalted using a HiPrep 26/10 desalting column, then lyophilized and stored at -80 °C until use. Alexa Fluor 647-labeled PG65 was aliquoted after SEC in PBSA containing 1 mM TCEP and stored at -80 °C until use. A labeled protein was mixed with the corresponding unlabeled protein at a molar ratio of 1:100 for sample preparation. Note that similar N-terminal labeling did not affect self-assembly properties of  $\alpha$ S and  $\alpha$ S linker mutants.<sup>12</sup>

### ***Time-course $\alpha$ S aggregation***

$\alpha$ S samples used for time-course aggregation analyses were prepared in a similar manner as outlined above in  $\alpha$ S sample preparation where incubation was necessary (i.e.  $\alpha$ S O and  $\alpha$ S F samples).  $\alpha$ S in solution at the beginning of incubation was found to be mostly monomeric, as determined by SEC<sup>12</sup>. These  $\alpha$ S samples were incubated at 37 °C with constant orbital shaking at 250 rpm in a New Brunswick Scientific Innova TM4230 incubator to initiate aggregation. Aliquots of  $\alpha$ S samples were removed at different time points during the aggregation process for measurements of RFC and ThT fluorescence as well as TEM imaging. Time-course aggregation of  $\alpha$ S in the presence of PG65 or pre-formed  $\alpha$ S oligomers ( $\alpha$ S O) was performed and examined similarly.

### ***8-anilino-1-naphthalenesulfonic acid (ANS) fluorescence***

$\alpha$ S solutions at a final concentration of 1.6  $\mu$ M were mixed with a solution of ANS at 16  $\mu$ M in PBSA. The ANS fluorescence of the samples was then immediately measured with an excitation wavelength of 350 nm, and emission was monitored at 475 nm.

### ***Circular dichroism (CD) spectroscopy***

Secondary structures of proteins in solution were determined by CD. Spectra were collected on a Jasco J-815 spectropolarimeter in the far-UV range with a 0.1 cm pathlength cuvette. The spectrum of the background (buffer only) was subtracted from the sample spectrum.

### ***Thioflavin T (ThT) fluorescence***

One point two  $\mu$ L of  $\alpha$ S solutions were mixed with 1  $\mu$ L of ThT solution at 1.0 mM and 197.8  $\mu$ L of PBSA. The ThT fluorescence of the samples was then immediately measured on a Photon Technology QuantaMaster QM-4 spectrofluorometer. The excitation wavelength was 440 nm, and emission was monitored at 487 nm.

### ***Dot blot assays***

One  $\mu$ g of proteins in aqueous buffer were applied to a nitrocellulose membrane and allowed to air dry at room temperature. Blocking, washing, incubation with primary and alkaline phosphatase-conjugated secondary antibodies, and chemiluminescent development were performed according to the manufacturer's protocols. A fluorescence dot blot assay using Alexa Fluor 647-labeled PG65 with cysteine to serine mutations as a probe was performed similarly, except for the omission of secondary antibody incubation. In this case, detection was achieved using the Molecular Dynamics Storm 840 molecular phosphorimager system housed at the NYU Chemistry Department Shared Instrumentation Facilities Center.

### ***Transmission electron microscopy (TEM)***

The aliquots (5  $\mu$ L) of a sample were placed on carbon membrane coated, glow discharged grids and negatively stained with 3% uranyl acetate in deionized water for 15 min. The samples were imaged on a Philips CM12 Transmission Electron Microscope (FEI Corp. Hillsboro, OR, USA) at 120 kV with a 4 k  $\times$  2.67 k GATAN digital camera located at the Image Core Facility of the Skirball Institute of Biomedical Sciences, NYU School of Medicine.

#### ***Size exclusion chromatography (SEC)***

Aggregation states of samples were analyzed with size exclusion chromatography (SEC) using a precision column prepacked with Superdex 200 (GE healthcare) on a GE FPLC system, as described previously.<sup>12</sup> Briefly, the mobile phase flow rate was set at 0.1 ml/min and elution peaks were detected by UV absorbance at 280 nm. The mobile phase buffer was PBSA used for preparation of  $\alpha$ S and protein probe samples. As reported previously<sup>26, 31</sup>,  $\alpha$ S monomers (MW: 14.5 kDa) eluted from Superdex 200 with the elution time corresponding to an apparent molecular weight of 60 kDa globular proteins. This is due to the effect of the natively unfolded conformation of  $\alpha$ S monomers on their Stokes radius as described previously.<sup>26, 31</sup>

#### ***In-gel fluorescence imaging***

In-gel fluorescence imaging of native-PAGE gels was carried out using the Storm 840 molecular phosphorimager system. For in-gel fluorescence imaging, Alexa Fluor 647-labeled PG65 prepared with a labeling ratio of ~0.1 was used directly without any further mixing with unlabeled PG65. Samples containing a mixture of Alexa Fluor 488-labeled  $\alpha$ S at a designated concentration + Alexa Fluor 647-labeled PG65 at 3.4  $\mu$ M or Alexa Fluor 488-labeled  $\alpha$ S only samples were prepared and incubated for 1 hr prior to running native-PAGE.

## REFERENCES

1. A. C. Ferreon, C. R. Moran, J. C. Ferreon and A. A. Deniz, *Angew Chem Int Ed Engl*, 2010, **49**, 3469-3472.
2. B. R. Martin, B. N. Giepmans, S. R. Adams and R. Y. Tsien, *Nat Biotechnol*, 2005, **23**, 1308-1314.
3. M. S. Celej, R. Sarroukh, E. Goormaghtigh, G. Fidelio, J. M. Ruyschaert and V. Raussens, *Biochem J*, 2012.
4. B. D. van Rooijen, M. M. Claessens and V. Subramaniam, *Biochim Biophys Acta*, 2009, **1788**, 1271-1278.
5. H. LeVine, 3rd, *Methods Enzymol*, 1999, **309**, 274-284.
6. R. Kayed, E. Head, J. L. Thompson, T. M. McIntire, S. C. Milton, C. W. Cotman and C. G. Glabe, *Science*, 2003, **300**, 486-489.
7. G. V. Semisotnov, N. A. Rodionova, O. I. Razgulyaev, V. N. Uversky, A. F. Gripas and R. I. Gilmanshin, *Biopolymers*, 1991, **31**, 119-128.
8. M. J. Volles, S. J. Lee, J. C. Rochet, M. D. Shtilerman, T. T. Ding, J. C. Kessler and P. T. Lansbury, Jr., *Biochemistry*, 2001, **40**, 7812-7819.
9. N. Cremades, S. I. Cohen, E. Deas, A. Y. Abramov, A. Y. Chen, A. Orte, M. Sandal, R. W. Clarke, P. Dunne, F. A. Aprile, C. W. Bertocini, N. W. Wood, T. P. Knowles, C. M. Dobson and D. Klenerman, *Cell*, 2012, **149**, 1048-1059.
10. A. Dusa, J. Kaylor, S. Edridge, N. Bodner, D. P. Hong and A. L. Fink, *Biochemistry*, 2006, **45**, 2752-2760.
11. L. Giehm, D. I. Svergun, D. E. Otzen and B. Vestergaard, *Proc Natl Acad Sci U S A*, 2011, **108**, 3246-3251.
12. M. Hernandez, S. Golbert, L. G. Zhang and J. R. Kim, *Chembiochem*, 2011, **12**, 2630-2639.
13. H. Y. Kim, M. K. Cho, A. Kumar, E. Maier, C. Siebenhaar, S. Becker, C. O. Fernandez, H. A. Lashuel, R. Benz, A. Lange and M. Zweckstetter, *J Am Chem Soc*, 2009, **131**, 17482-17489.
14. O. M. El-Agnaf, S. A. Salem, K. E. Paleologou, L. J. Cooper, N. J. Fullwood, M. J. Gibson, M. D. Curran, J. A. Court, D. M. Mann, S. Ikeda, M. R. Cookson, J. Hardy and D. Allsop, *FASEB J*, 2003, **17**, 1945-1947.
15. A. L. Rucker and T. P. Creamer, *Protein Sci*, 2002, **11**, 980-985.
16. I. Gokce, R. W. Woody, G. Anderluh and J. H. Lakey, *J Am Chem Soc*, 2005, **127**, 9700-9701.
17. F. Eker, K. Griebenow and R. Schweitzer-Stenner, *J Am Chem Soc*, 2003, **125**, 8178-8185.
18. W. B. Rippon and A. G. Walton, *Biopolymers*, 1971, **10**, 1207-1212.
19. Y. Hu, B. Su, H. Zheng and J. R. Kim, *Mol Biosyst*, 2012, **8**, 2741-2752.
20. M. J. Roberti, C. W. Bertocini, R. Klement, E. A. Jares-Erijman and T. M. Jovin, *Nat Methods*, 2007, **4**, 345-351.
21. J. M. Estevez and C. Somerville, *Biotechniques*, 2006, **41**, 569-570, 572-564.
22. K. A. Conway, J. D. Harper and P. T. Lansbury, *Nat Med*, 1998, **4**, 1318-1320.
23. E. A. Greenbaum, C. L. Graves, A. J. Mishizen-Eberz, M. A. Lupoli, D. R. Lynch, S. W. Englander, P. H. Axelsen and B. I. Giasson, *J Biol Chem*, 2005, **280**, 7800-7807.
24. M. Tashiro, M. Kojima, H. Kihara, K. Kasai, T. Kamiyoshihara, K. Ueda and S. Shimotakahara, *Biochem Biophys Res Commun*, 2008, **369**, 910-914.
25. B. Fauvet, M. K. Mbefo, M. B. Fares, C. Desobry, S. Michael, M. T. Ardah, E. Tsika, P. Coune, M. Prudent, N. Lion, D. Eliezer, D. J. Moore, B. Schneider, P. Aebischer, O. M. El-Agnaf, E. Masliah and H. A. Lashuel, *J Biol Chem*, 2012, **287**, 15345-15364.
26. P. H. Weinreb, W. Zhen, A. W. Poon, K. A. Conway and P. T. Lansbury, Jr., *Biochemistry*, 1996, **35**, 13709-13715.
27. V. N. Uversky, J. Li, P. Souillac, I. S. Millett, S. Doniach, R. Jakes, M. Goedert and A. L. Fink, *J Biol Chem*, 2002, **277**, 11970-11978.
28. D. B. Wetlaufer, *Adv. Protein Chem.*, 1962, **17**, 303-390.
29. B. Krishnan and L. M. Gierasch, *Chem Biol*, 2008, **15**, 1104-1115.
30. D. E. Ehrnhoefer, J. Bieschke, A. Boeddrich, M. Herbst, L. Masino, R. Lurz, S. Engemann, A. Pastore and E. E. Wanker, *Nat Struct Mol Biol*, 2008, **15**, 558-566.
31. R. A. Fredenburg, C. Rospigliosi, R. K. Meray, J. C. Kessler, H. A. Lashuel, D. Eliezer and P. T. Lansbury, Jr., *Biochemistry*, 2007, **46**, 7107-7118.